Available online at www.sciencedirect.com
ScienceDirect
Earth and Planetary Science Letters 258 (2007) 293–306
EPSL
www.elsevier.com/locate/epsl

High-resolution magnetostratigraphy of the Neogene Huaitoutala section in the eastern Qaidam Basin on the NE Tibetan Plateau, Qinghai Province, China and its implication on tectonic uplift of the NE Tibetan Plateau

Xiaomin Fang [a,b,*], Weilin Zhang [a], Qingquan Meng [b], Junping Gao [b], Xiaoming Wang [c], John King [d], Chunhui Song [b], Shuang Dai [b], Yunfa Miao [b]

[a] *Center for Basin Resource and Environment, Institute of Tibetan Plateau Research, Chinese Academy of Sciences, P. O. Box 2871, Beilin North Str. 18, Beijing 100085, China*
[b] *Key Laboratory of Western China's Environmental Systems, Ministry of Education of China & College of Resources and Environment, Lanzhou University, Gansu 730000, China*
[c] *Department of Vertebrate Paleontology, Natural History Museum of Los Angeles County, 900 Exposition Boulevard, Los Angeles, CA 90007, USA*
[d] *Graduate School of Oceanography, University of Rhode Island, URI Bay Campus Box 52, South Ferry Road, Narragansett, RI 02882-1197, USA*

Received 31 December 2006; received in revised form 23 March 2007; accepted 23 March 2007
Available online 31 March 2007
Editor: R.D. van der Hilst

Abstract

The closed inland Qaidam Basin in the NE Tibetan Plateau contains possibly the world's thickest (~12,000 m) continuous sequence of Cenozoic fluviolacustrine sedimentary rocks. This sequence contains considerable information on the history of Tibetan uplift and associated climatic change. However, work within Qaidam Basin has been held back by a paucity of precise time constraints on this sequence. Here we report on a detailed paleomagnetic study of the well exposed 4570 m Huaitoutala section along the Keluke anticline in the northeastern Qaidam Basin, where three distinct faunas were recovered and identified from the middle Miocene through Pliocene. Constrained by these faunal ages, the observed thirty-three pairs of normal and reversed polarity zones can be readily correlated with chrons 2n-5Br of the GPTS. This study assigns the age of the section to the interval between ca. 15.7 Ma to 1.8 Ma. In addition, the widely used stratigraphic units the Xia Youshashan, Shang Youshashan, the Shizigou and Qigequan Formations were formed at >15.3 Ma, 15.3–8.1 Ma, 8.1–2.5 Ma and <2.5 Ma, respectively. We obtained a very high average sedimentation rate of ~33 cm/ka over the entire interval 15.7 to 1.8 Ma. Furthermore, the average sedimentation rate is punctuated by three intervals of persistent rapid increases starting at about ~14.7 Ma, 8.1 Ma and 3.6 Ma. These intervals are interpreted as times of rapid uplift and fast exhumation of the NE Tibetan Plateau.

Keywords: magnetostratigraphy; Neogene; Qaidam Basin; NE Tibetan Plateau

* Corresponding author. Center for Basin Resource and Environment, Institute of Tibetan Plateau Research, Chinese Academy of Sciences, P. O. Box 2871, Beilin North Str. 18, Beijing 100085, China. Tel.: +86 10 6284 9697; fax: +86 10 6284 9886.
E-mail address: fangxm@itpcas.ac.cn (X. Fang).

0012-821X/$ - see front matter © 2007 Published by Elsevier B.V.
doi:10.1016/j.epsl.2007.03.042

1. Introduction

The Qaidam Basin (~850 km long × 150–300 km wide = ~121,000 km^2) is the largest basin on the northeastern Tibetan Plateau. It is bounded by the Qiman Tagh–Kunlun Shan (Mts.) to the south, the Altyn Tagh (Mts.) to the northwest, the Qilian Shan (Mts.) to the northeast and the Ela Shan (Mts.) to the east. It has an average elevation of 3000 m above sea level, in contrast to the surrounding mountains with elevations of 4000–5000 m (Fig. 1). It has been interpreted to have been a closed inland basin since the Paleocene and is filled with a maximum thickness of ~12,000 m of Cenozoic sediments (the thickest known section of Cenozoic continent sediments) shed from the surrounding mountains [1–3]. It is located in the arid region of North China, but is still affected by the front of the Asian monsoon. The sedimentary record of this basin attracts considerable attention because: (1) it contains a great potential record of the initiation and development of the Asian monsoon and of Asian aridification [4–6]; (2) it provides a record of the ongoing growth of the Tibetan Plateau flat surface through the infilling of basins [7,8]; (3) it provides a typical example for Cenozoic crustal detachment [9,10]; and (4) it provides a record of the deformation and uplift of the Kunlun Shan and the Qilian Shan, especially the activation of the huge (1500 m long) strike–slip Altyn Tagh fault that has been thought to be a key boundary to transfer the deformation caused by the collision of India with Asia by continental extrusion [8,11,12]. Several tectonic models predict that either the Qaidam Basin and the northeastern Tibetan Plateau are the most recently deformed and most tectonically active part of Tibet [7,8,10], or comprise the entirety of the Cenozoic deformed block [13]. Unfortunately, until our work, we have not had accurate chronology and paleoenvironmental and tectonic records from the Qaidam Basin to either to reconstruct the histories of the Asian monsoon and Asian desertification, or for testing the tectonic models. This lack of an accurate chronology is largely caused by a previous paucity of mammalian fossils or other means of obtaining geochronology from the thick Cenozoic sedimentary sequences.

This barrier was slowly breached by a steady stream of discoveries of fossil mammals in the east Qaidam Basin since 1998 [14,15] that followed early discoveries

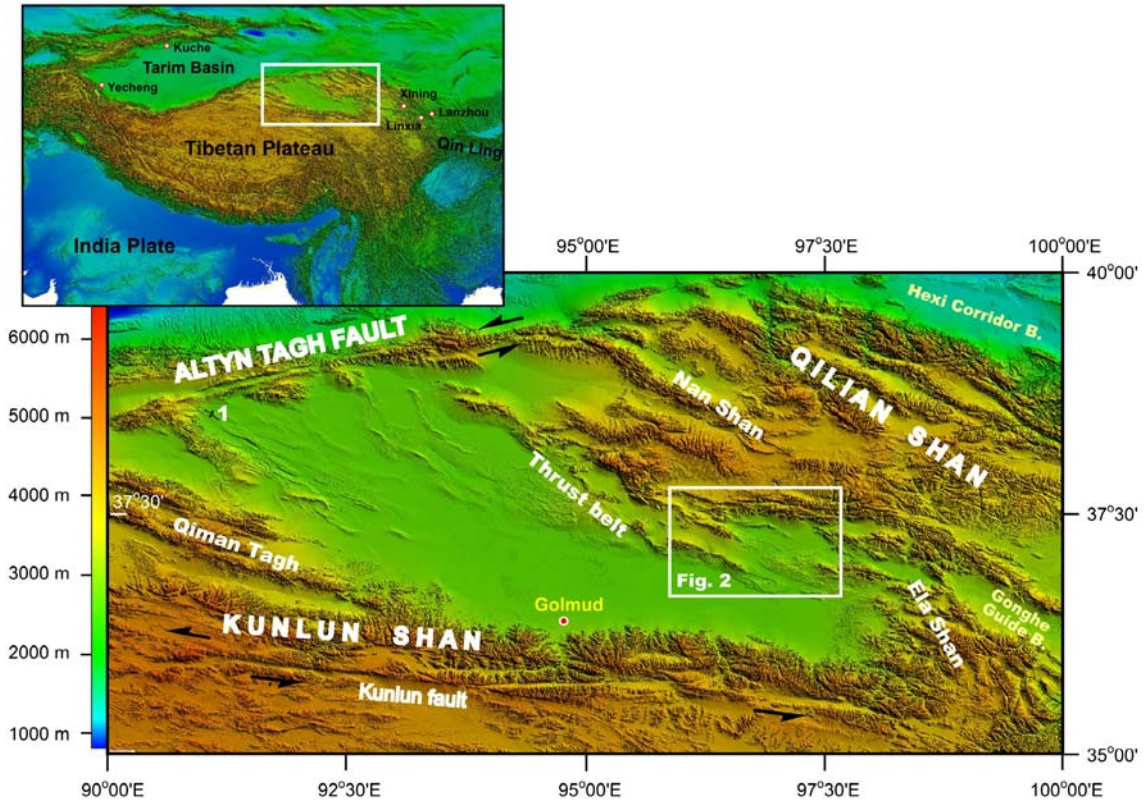

Fig. 1. DEM presentation of the geomorphology of the Qaidam Basin and its surrounding mountains. 1: Honggouzi anticline; Thrust belt: North Qaidam marginal thrust belt.

by a Swedish paleontologist, Birger Bohlin. With few exceptions, the mammal sites are located in the northeastern Qaidam Basin in the vicinity of Delingha and Huaitoutala and span the stratigraphic interval between the middle Miocene and Pliocene [16,17] (Fig. 8). We now have sufficient mammal finds that are age diagnostic to provide chronological constraints on a number of fossiliferous sections. Encouraged by these findings, we choose the Huaitoutala section, 10 km south of the village of Huaitoutala, for detailed paleomagnetic studies, because it bears seven layers of fossil mammals containing components of most of the fossil mammal groups found in the region (Fig. 2). A chronology based on an integrated study of the mammalian fossils and paleomagnetic polarity reversals obtained from the relatively long and continuous section offers the best resolution possible for a continental setting that does not contain volcanic rocks that can be radiometrically dated. The absence of dateable volcanic rocks is typical of much of Asia during the Cenozoic [16].

2. Geologic setting and stratigraphy

The high relief contrast between the depressed Qaidam Basin and highly uplifted surrounding mountains is controlled by the large boundary faults between them [1,2,11,12] (Fig. 1). The north Kunlun fault, derived from the Kunlun fault belt along the Qiman Tagh and the Kunlun Shan, bounds the southern margin of the Qaidam Basin. The Kunlun fault runs roughly east–west for about 1100 km and is a major strike–slip fault thought to absorb and transfer deformation imposed by the collision of India with Asia [11,12] (Fig. 1). The impressive 1500-km long, NE–SW left-lateral strike–slip Altyn Tagh fault cuts through the northwestern margin of the Qaidam Basin. Between ~350–400 km [18–20] and ~500–700 km displacement [21,22] is thought to have taken place along the fault. This displacement has caused not only the depression and deformation of the Qaidam Basin and formation of the Altyn Tagh mountains, but has also transferred much of the deformation into the broad region of the Nan Shan–Qilian Shan, resulting in an intense uplift of the region [2,8,11–13,23] (Fig. 1). The northern margin of the Qaidam Basin is bounded by the Nan Shan and the Zongwulong Shan faults (also called the south marginal fault of Qilian Shan; F_1 in Figs. 2 and 3) that run in a NWW–SEE direction. These faults are not only geometrically but also dynamically linked with the Altyn Tagh fault to absorb the transferred deformation and have caused strong deformation and uplift of the Nan Shan. This transfer has formed a broad thrust belt (ca. 440 km long × 65 km wide = 30,000 km^2) in the northern margin of the Qaidam Basin, called the north Qaidam marginal thrust belt (NQMTB), which parallels the southern margin of the Qilian Shan [1,2] (Fig. 1). A series of north-dipping thrusts and their associated south-dipping backthrusts can be clearly observed in the surface, satellite and DEM images and seismic profiles within the NQMTB in the study area. These thrusts and backthrusts fall roughly into four groups of tectonic units, the Delingha depression, the Olonbuluk upheaval, the South Olonbuluk depression, and the Emonike upheaval (Figs. 1–3). To the north and south of the NQMTB are the tectonic units of the Qilian Shan and the Plio-Quaternary depocenter of the Qaidam Basin, the Huobusun depression with a maximum depth of ~12,000 m [1,2]. The Emonike upheaval is the front of the north Qaidam thrust belt, and exposes largely Devonian volcanic detritus and sea shelf limestone with some Carboniferous sandstone and limestone and Jurassic sandstone and mudstone with coals (Fig. 2). Field observations and seismic data show that the backthrusts F_4 and F_3 of front thrust F_7 have caused a south tilted depression, the south Olonbuluk depression. The long-axis of the depression deepens southwestwards with a maximum depth of 3500–400 m occurring in the area of the Tuxi to Wulan anticlines to the southeast of Tuosu Hu (Lake) (Figs. 2 and 3). These data further show that the Olonbuluk upheaval is a thin bedrock slab that was probably also uplifted by the larger backthrust F_2 of front thrust F_7. This fault backthrusts the southern margin of the Delingha depression northward, to face the opposite thrust fault F_1 that thrusts the northern margin of the Delingha depression southward. This tectonic activity has probably given rise to the formation of the very deep NWW–SEE trending Delingha depression (~3687 km^2) that contains Cenozoic sediments that are over 6000 m thick (Figs. 2 and 3). Furthermore, the strong backthrusting of F_2 has caused the backward propagation fault F_2 that thrusts and folds the Cenozoic stratigraphy to the north of the Olonbuluk Shan to form the Keluke anticline (Figs. 2 and 3).

The Cenozoic stratigraphy in the Qaidam Basin has historically been divided into six formations with assigned ages. These are (in upward sequence) the Lulehe Fm. (Paleocene to Eocene, E_{1-2}), the Xia Ganchaigou Fm. (Oligocene, E_3), the Shang Ganchaigou Fm. (early Miocene, N_1), the Xia Youshashan Fm. (mid Miocene, N_2^1), the Shang Youshashan Fm. (late Miocene, N_2^2), the Shizigou Fm. (Pliocene, N_2^3) and the Qigequan Fm. (early Pleistocene, Q_1). This age assignment is largely based on pollen and ostracode analyses and has been widely accepted for geologic and tectonic studies and

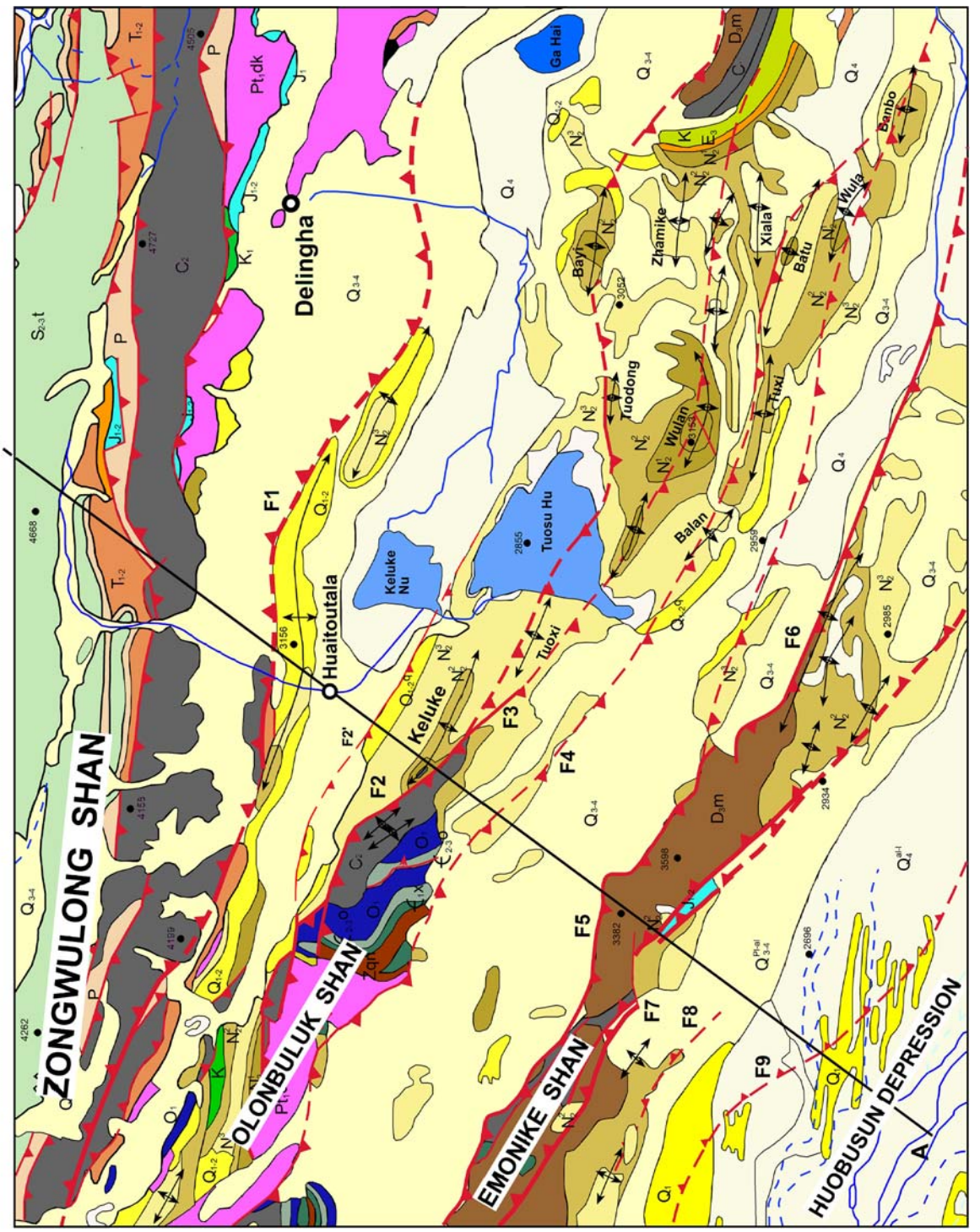

Fig. 2. Geologic map of the eastern part of the north Qaidam marginal thrust showing the fault system and locations of the Huaitoutala section along the north limb of the Keluke anticline. See Fig. 1 for its location. Solid red line: surface fault; broken red line: sub-surface fault given by satellite images and seismostratigraphy.

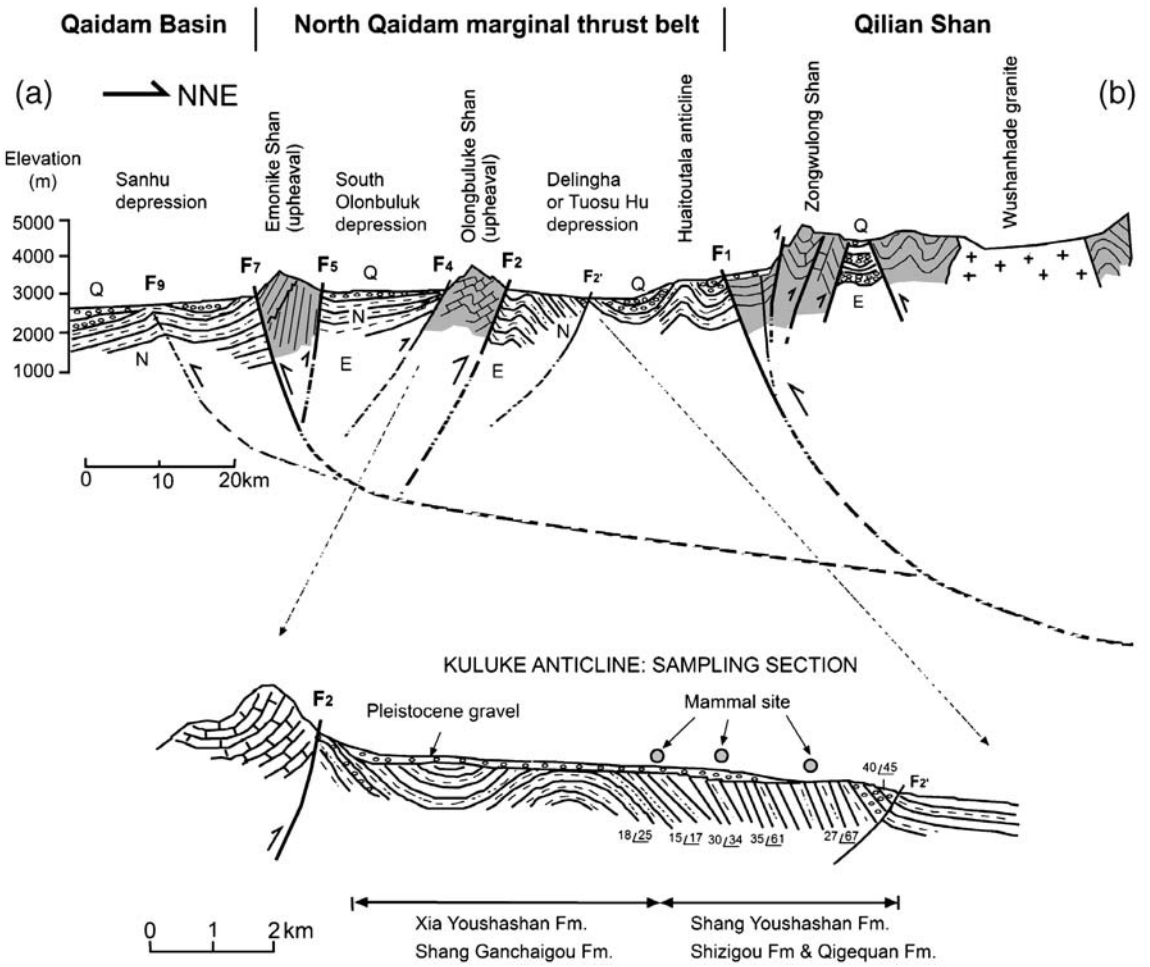

Fig. 3. Cross-section of A–B in Fig. 2 with locations for fossil mammal sites. Note the lower part of fault is mostly schematic and is not plotted in real vertical scale; the profile is vertically exaggerated; selected dip directions and dips are shown.

lithostratigraphic correlation [1–3]. The Lulehe Fm. is only found in the western Qaidam Basin along the margins of the Qiman Tagh–Kunlun Shan, the Altyn Tagh and the Nan Shan. The lithology is predominantly purple red and dark red alluvial conglomerate and gravelly sandstone intercalated with some sandy mudstone and siltstone along the basin margin and a distal facies of shallow lake siltstone and mudstone toward the basin center. It superimposes unconformably upon Early Cretaceous and other older rocks. The Xia Ganchaigou Fm. has a larger distribution area than the Lulehe Fm. and is characterized by alternate brown red alluvial to fluvial conglomerate, gravelly sandstone and brown, yellow-green sandy mudstone in the lower part and playa brown siltstone and gray mudstone in the upper part with thick salt and gypsum deposits in the depocenter close to the Altyn Tagh fault. The Shang Ganchaigou Fm. covers the whole basin and is largely interbedded multi-colored (brown to gray-green) lacustrine sandstone, siltstone and mudstone intercalated with marl and nodular limestone. The Xia Youshashan Fm. appears over the entire basin and consists largely of gray yellow and brown sandstone to mudstone with some oolite marl at the basin center and fine conglomerate and sandstone at the basin margin. The Shang Youshashan Fm. is dominated by gray/yellow-green and light brown conglomerate, gravelly sandstone, siltstone and mudstone. It contacts conformably with the underlying Xia Youshashan Fm. at the basin center but unconformably at the basin margins, especially along the western margin. The Shizigou Fm. is mostly conglomerate to sandstone intercalated with siltstone in the basin margin and yellow-gray calcareous sandy mudstone intercalated with blue-gray sandstone and gravely sandstone. It also contacts conformably with the underlying Shang Youshashan Fm. at the basin center but unconformably

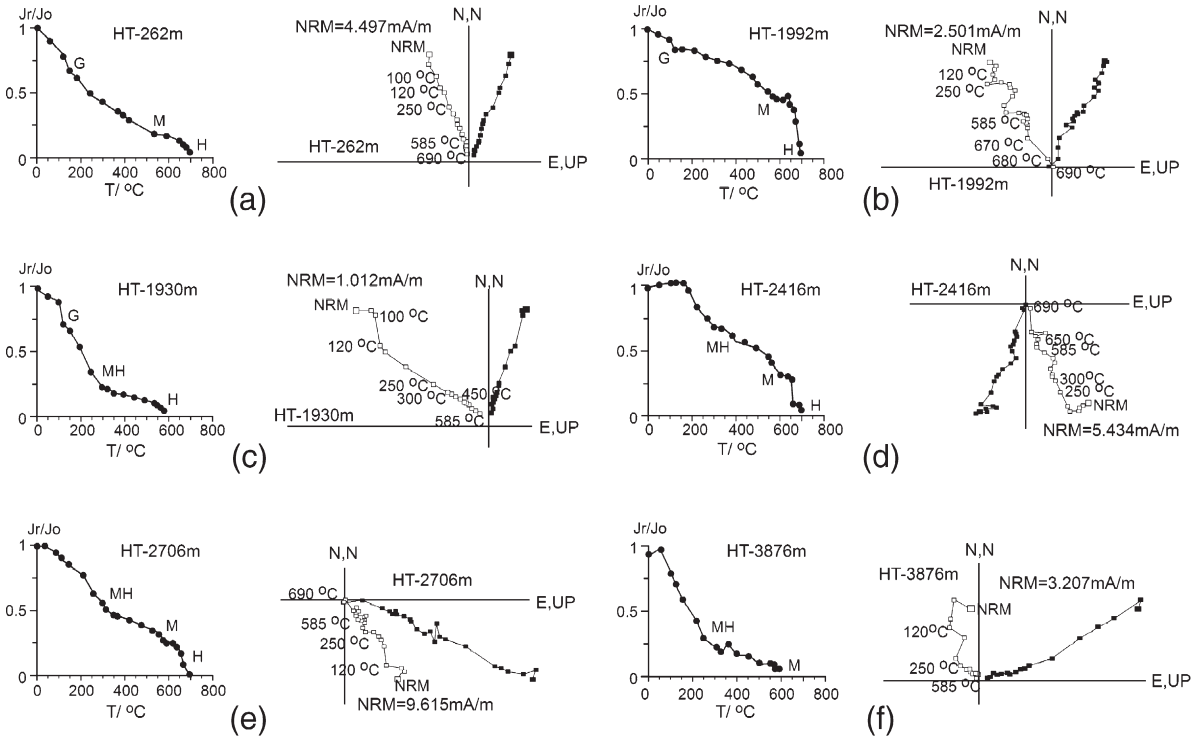

Fig. 4. Representative thermal orthogonal demagnetization diagrams for samples from the Huaitoutala section (directions are original data in geographic coordinates). Open (closed) symbols represent vertical (horizontal) projections; intensities are given in mA/m. NRM, natural remanent magnetization; G, geothite; MH, maghemite; M, magnetite; H, hematite.

at the basin margins. The Qigequan Fm. is a distinctively thick gray conglomerate intercalated with sandstone and sandy siltstone–mudstone covering most of the basin. Only in the depocenter at the middle to eastern part of the basin does it change to dark gray mudstone intercalated with siltstone and muddy sandstone [1,2,24].

Our paleomagnetic section lies along the northern limb of the Keluke anticline against the northern edge of the Olonbuluk Shan, about 10 km south of Huaitoutala Town (Fig. 2). It is a 4570-m exposed outcrop of the middle Miocene to Quaternary sedimentary rocks consisting of the Xia Youshashan Fm., Shang Youshashan Fm., Shizigou Fm. and Qigequan Fm. (Fig. 3). The Xia Youshashan Fm. has an exposure of only 100 m, characterized by fine-grained sedimentary rocks of siltstone, mudstone and marl. The Shang Youshashan Fm. is 2250 m thick (from 100 m to 2350 m) and consists mainly of conglomerate and sandstone intercalated with siltstone for most of the stratigraphy and siltstone and mudstone in the uppermost part. The Shizigou Fm. is 1750 m thick (from 2350 m to 4100 m), and is dominated by thick sandstone intercalated with some mudstone. The Qigequan Fm. is only 470 m thick and is mainly conglomerate intercalated with thin sandy siltstone and mudstone (Fig. 8a).

3. Sampling and measurements

Oriented block samples of roughly $10\times10\times8$ cm were taken at intervals of 2–5 m depending on the availability of a suitable lithology at each level (site). These block samples were then cut into three oriented cubic specimens of $2\times2\times2$ cm in the laboratory to form three parallel sets of samples for cross-calibration measurements. A total of 1650 block samples and 1650×3 specimens were obtained.

Systematic stepwise thermal demagnetizations (in fifteen to twenty discrete steps between ~25 °C and 690 °C at intervals of 50 °C below 550 °C and 10–20 °C above it) were done on the first set of specimens and the 240 pilot samples of the second set of the specimens. Remanent intensities and directional measurements were done on a 2G Enterprises magnetometer in a magnetically shielded room, first in the Paleomagnetism Laboratory of the Institute of Geology and Geophysics (Chinese Academy of Sciences) and the Paleomagnetic and Rock Magnetic Laboratory of the Key Laboratory of Western China's Environmental

Systems (Ministry of Education of China) in Lanzhou University, and then at the Graduate School of Oceanography, University of Rhode Island. Based on these results, only six to eight steps for temperatures between 350 °C and 675 °C were applied to the remaining specimens of the second set.

The intensity of the natural remanent magnetization (NRM) of the clastic sedimentary samples is 1.5×10^{-2} to 1.6×10^{-3} A/m for mudstone and siltstone, and 0.6×10^{-2} to 0.8×10^{-3} A/m for sandstone. Representative thermal demagnetization diagrams are shown in Fig. 4. Most samples show simple demagnetization behavior. Below 50–100 °C, a viscous remanent magnetization (VRM) is readily removed (Fig. 4). Between 100 and 120 °C, many samples show a clear decrease in magnetization , accompanied by a clear change of remanent direction that indicates the removal of a secondary remanent magnetization (SRM) stored by goethite (Fig. 4a, b, c). Most samples show a low unblocking temperature component that can be removed easily at 250 °C (Fig. 4). Above this temperature, a characteristic magnetization (ChRM) is clearly isolated and decays nearly linearly to the origin. Three obvious rapid decays of the magnetization were observed for most samples at about 350 °C, 580 °C and 660–690 °C, indicative of the presence of maghemite, magnetite and hematite that act as major ChRM-carriers (Fig. 4).

ChRM component directions have been calculated for all samples using Principal Component Analysis. Remanence directions of the specimens generally agreed between the three laboratories unless the specimens were unstable and showed noisy demagnetization behavior (~10% of the total, mostly from coarse sandstones). The final ChRM direction at each site was obtained by Fisher averaging of the directions from the two sets of specimens. Specimens not included in our magnetostratigraphic analysis were rejected based on three criteria. (1) ChRM directions could not be determined because of ambiguous or noisy orthogonal demagnetization diagrams. (2) ChRM directions revealed maximum angular deviation (MAD) angles greater than 15°. (3) Specimens revealed magnetizations with virtual geomagnetic pole (VGP) latitude values less than 30°. A total of 495 horizontal levels in the column (30%) were excluded. The final remanent directions are averaged for each level and then are used to calculate VGPs that are plotted as a function of thickness after various paleomagnetic tests (Figs. 5–7).

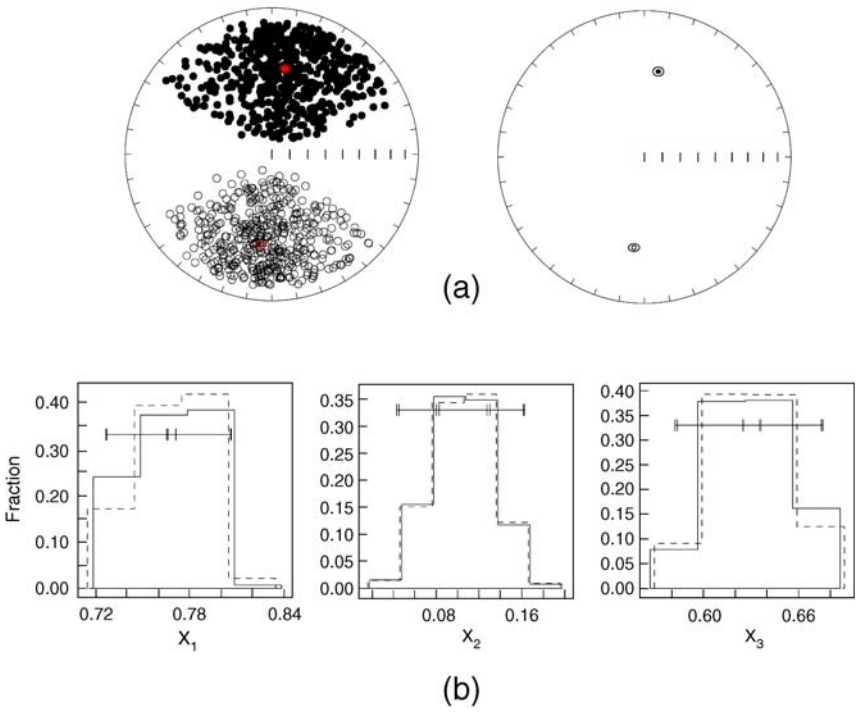

Fig. 5. (a) Equal-area projections of the characteristic remanent magnetization (ChRM) directions and mean directions (with oval of 95% confidence) for the Huaitoutala section determined with the bootstrap method (Tauxe [25]). Downward (upward) directions are shown as filled (open) circles. (b) Bootstrap reversal test diagram. Reversed polarity directions have been inverted to their antipodes to test for a common mean for the normal and reversed magnetization directions. The confidence intervals for all components overlap, indicating a positive reversal test. (For interpretation of the references to colour in this figure legend, the reader is referred to the web version of this article.)

4. Magnetostratigraphy

All the accepted ChRM directions of the Huaitoutala section from the Keluke anticline are used for a reversal test after tilt correction. An equal area projection of these ChRM directions shows that they record signals from the dipole of the earth's magnetic field (Fig. 5a). A statistical bootstrap technique [25] has been used to test whether the distributions of the ChRM vectors are possibly non-Fisherian, and to characterize the associated uncertainties for both normal and reversed ChRM directions (Fig. 5b). The histograms of the Cartesian coordinates of bootstrapped means [25] allow us to determine a 95% level of confidence (ovals around the means in Fig. 5a) and to demonstrate that the bootstrap reversal test is positive (Fig. 5b).

The large change in bedding tilt along the section nearly orthogonally transecting the north limb of the Keluke anticline (Fig. 3) provides an opportunity for a fold test [26,27]. 248 representative high quality (MAD < 5) site-mean ChRMs from different parts of the section were used for a calculation by the method of McElhinny [26], which indicates a positive fold test with the tilt-dependent dispersed ChRM directions tending to cluster together around their antipolar means (Fig. 6).

Furthermore, a jackknife technique [28] was used to quantify the reliability of the magnetostratigraphy. The jackknife parameter (J) obtained for the accepted specimen-mean directions has a value of −0.3, which falls within the range of 0 to −0.5 recommended for a robust magnetostratigraphic data set by Tauxe and Gallet [28]. This result indicates that sampling of the section has recovered more than 95% of the true number of polarity intervals (Fig. 7).

Fig. 8 shows a thickness vs. VGP plot of all the accepted and tested ChRM directions. It shows that there are a total of 33 normal and 33 reversed polarity intervals recorded in the Huaitoutala section, marked as N1–N33 and R1–R33, respectively (Fig. 8). The observed polarities can be correlated well with chrons 2n-5Br of the Geomagnetic Polarity Time Scale (GPTS) of Cande and Kent [29] for most of the section. First, the strikingly long normal intervals N3–N4, N18 and N29–31 can be readily correlated to the characteristic long normal

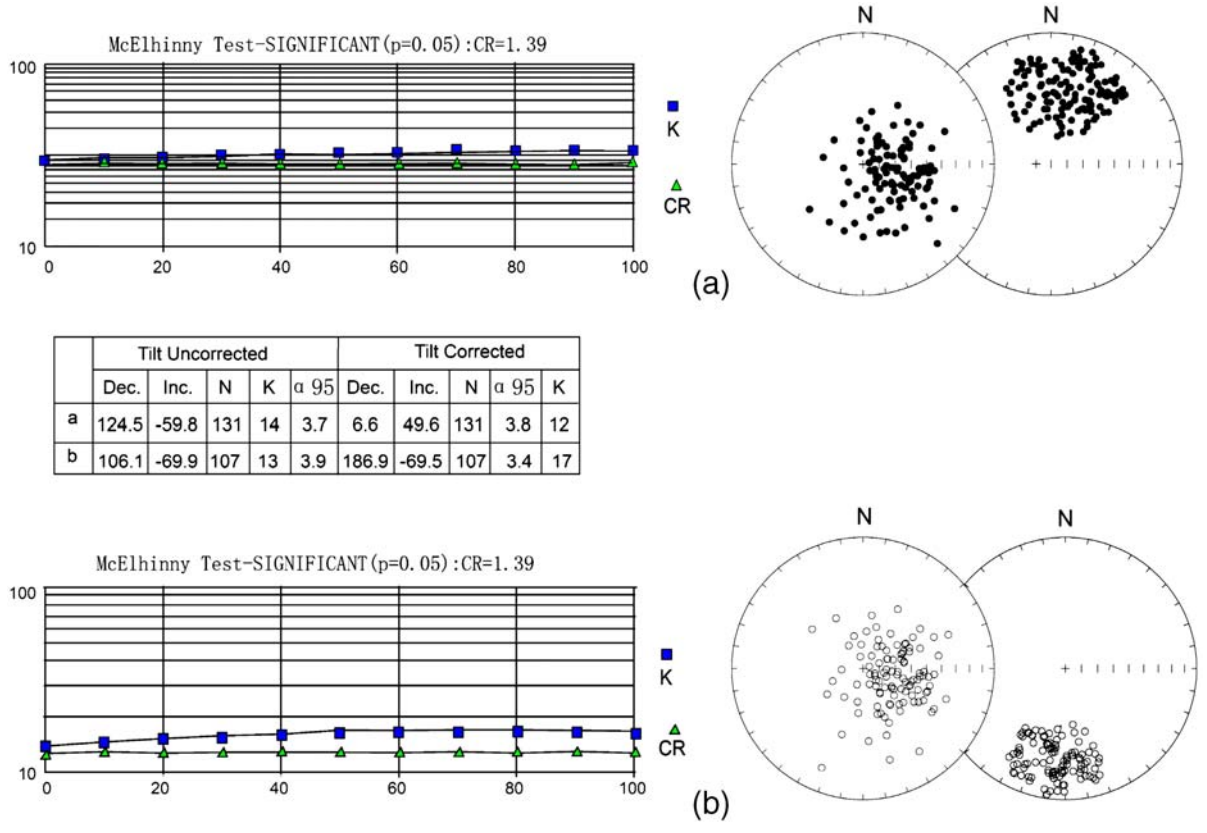

	Tilt Uncorrected					Tilt Corrected				
	Dec.	Inc.	N	K	α 95	Dec.	Inc.	N	α 95	K
a	124.5	-59.8	131	14	3.7	6.6	49.6	131	3.8	12
b	106.1	-69.9	107	13	3.9	186.9	-69.5	107	3.4	17

Fig. 6. Diagram showing a positive fold test of the 248 representative high quality site-mean ChRMs from different parts of the section using method by McElhinny [26]. (For interpretation of the references to colour in this figure legend, the reader is referred to the web version of this article.)

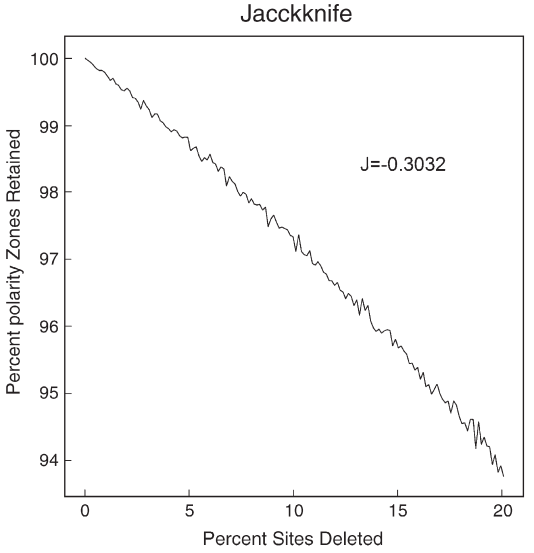

Fig. 7. Magnetostratigraphic jackknife analysis (Tauxe and Gallet [28]) for the Huaitoutala section. The plot indicates the relationship between average percent of polarity zones retained and the percentage of sampling sites deleted, where the slope J is directly related to the robustness of the results. The obtained slopes J have values of −0.3032 in the study section, which predicts that the section has recovered more than 95% of the true number of polarity intervals.

chrons 2n (the Gauss Normal Polarity Chron), 5n and 5ACn-5ADn, respectively. Then, the short normal intervals N5–N8 of nearly equal duration are straightforwardly correlated to the four short normal events of chron 3n in the Gilbert Reversed Polarity Chron, as the Cochiti, Nunivak, Sidufjall and Thvera subchrons, respectively (Cande and Kent [29]); N9–10 to chron 3An; N13–14, N16, N21–22, N27–28 and N32–33 to chron 4n, 4An, 5An, 5ABn and 5ABn, respectively (Fig. 8). The two clearly normal intervals N1 and N2 at the top of the section are regarded as analogs of the Reunion and Olduvai subchrons (2r.1n and 2n) in the Matuyama Reversed Polarity Chron, because of the persistent occurrence of very coarse sedimentary rocks (conglomerate and coarse sandstone) that indicate a fast depositional rate (Fig. 8). Thus, the whole section was estimated to have formed between about 15.7 Ma and 1.8 Ma.

The fossil mammals found in the lower, middle and upper parts of the section provide robust constraints on our interpretation of the observed polarities. These mammals fall into three faunas in the middle Miocene, late Miocene, and early Pliocene, respectively (Wang et al., in preparation) (Table 1 and Fig. 8b). The Olonbuluk Fauna contains species of primitive deer *Lagomeryx* and *Stephanocemas*, as well as rhinos such as *Acerorhinus tsaidamensis* [15]. These taxa commonly occur in the middle Miocene of north China and are typical elements of the Tunggurian Land Mammal Age [30]. The Tuosu Fauna features possibly the earliest occurrence of a *Hipparion* horse [16], as well as left over elements from the middle Miocene such as the *Dicroceros* deer. Presence of the three-toed horse undoubtedly indicates a late Miocene age and the Tuosu Fauna thus falls in the Baodean Land Mammal Age. The Huaitoutala Fauna currently contains small mammals only. It contains such typical Pliocene north China components as *Orientalomys/Chardinomys* and *Mimomys* and belongs to the Yushean Land Mammal Age. Thus defined, the lower Olonbuluk Fauna is estimated to occur in 12.5–13.8 Ma, the middle Tuosu Fauna at ~11.4–9.5 Ma, and the upper Huaitoutala fauna at ~4.8 Ma (Fig. 8).

Fig. 9 presents a thickness-vs.-age plot of the main chrons. It shows a linear relationship between the sampling thicknesses and chron ages that agrees to a first order (long-term change) with the lithologic change, which lends further support to our interpretation.

Thus, the complete Shang Youshashan Fm. and Shizigou Fm. are determined to have formed in the intervals 15.3–8.1 Ma and 8.1–2.5 Ma, respectively. The Xia Youshashan Fm. and Qigequan Fm. are older and younger than 15.3 Ma and 2.5 Ma, respectively.

5. Tectonic implications

Based on the magnetostratigraphy, the average sedimentation rate of the Huaitoutala section was calculated at about 33 cm/ka. This very high rate is punctuated by three large persistent increases that started at about 14.7 Ma, 8.1 Ma and 3.6 Ma. We interpret these unusually high sedimentation rate changes as records of three episodes of rapid tectonic uplift and fast exhumation and denudation (events T1 to T3) of the NE Tibetan Plateau for the following reasons (Fig. 9). First, early Cenozoic sedimentation rates are estimated at about 4–8 cm/ka in the Qaidam Basin and the Tarim and Hexi Corridor Basins to the west and north of the Qilian Shan [31–33], and as low as ~2–3 cm/ka in the Xining Basin in the eastern Qilian Shan and Lanzhou–Linxia Basins [34–37] (see Fig. 1 for localities). Second, in the late Cenozoic, sedimentation rates in these areas are generally three to four times higher than the early Cenozoic [33,36,38,39] with maximum rates over 70–80 cm/ka clearly associated with tectonic deformation and uplift in the Gonghe–Guide Basin and Tarim Basin [40,41] (Fig. 1). Third, the late Cenozoic sedimentation rate increase also broadly agrees with the tectonic evolution of a late rapid deformation and uplift

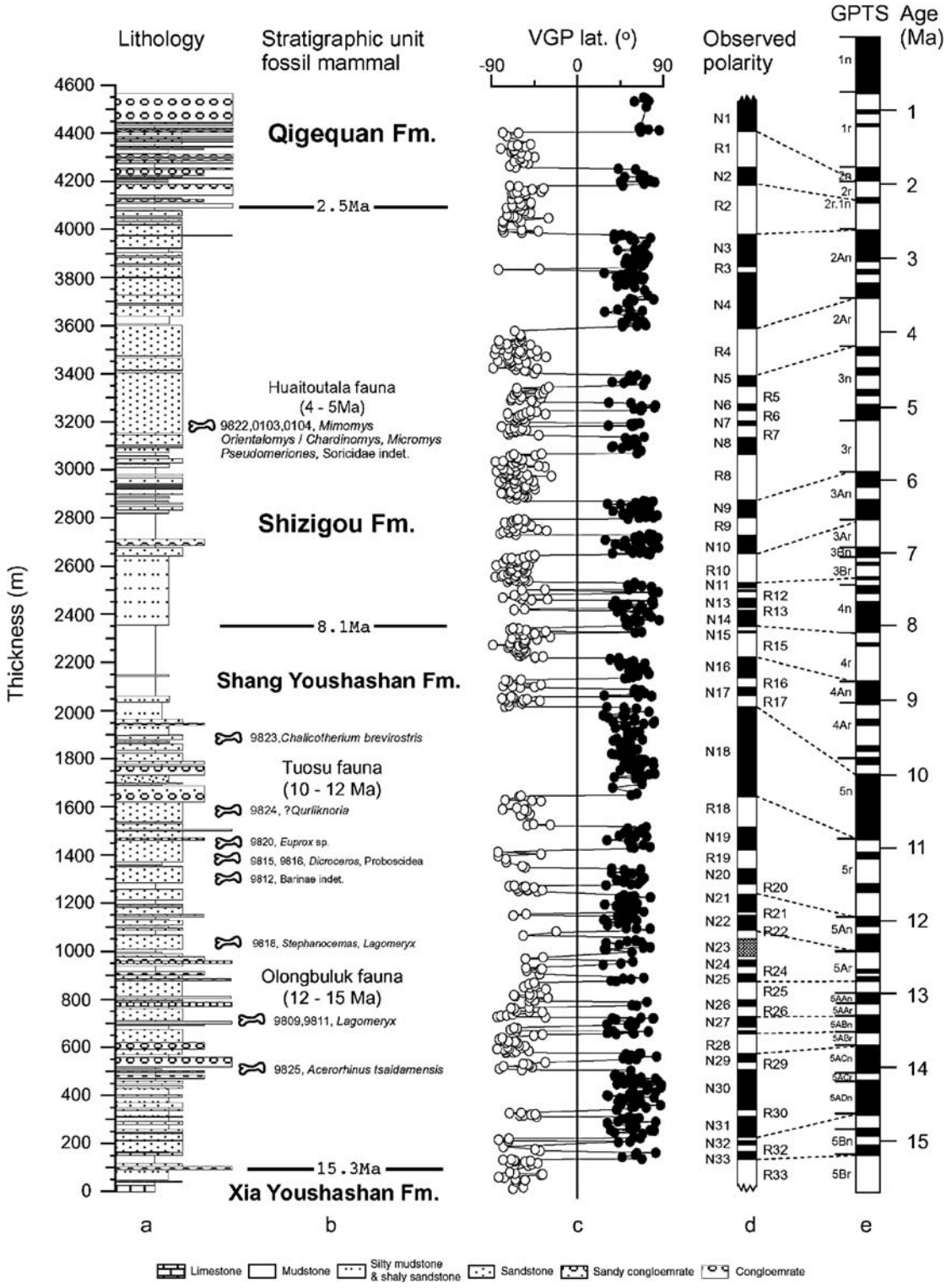

Fig. 8. Magnetostratigraphic results versus lithostratigraphic position for the Huaitoutala section. Sites and main components of fossil mammals found along the section are plotted on the right side of the stratigraphic column for general age constraint. Identification of the mammals and their significance will be published by another paper by Xiaomin Wang and others. VGP: virtual geomagnetic polarity; GPTS: geomagnetic polarity time scale of Cande and Kent [29]. Shaded polarity: suspected polarity most likely due to not sampling of a fresh surface.

Table 1
Mammalian faunas found in the Huaitoutala magnetic section and the nearby Tuosu Nor section

Name of fauna and component	Suggested age
Olongbuluk Fauna	Middle Miocene (12–15 Ma)
Acerorhinus tsaidamensis, CD9825	
Lagomeryx tsaidamensis, CD9811, CD9818	
Stephanocemas sp., CD9818	
Tuosu Fauna	Late Miocene (10–12 Ma)
Dicroceros sp., CD9815	
Euprox sp., CD9820	
?*Qurliknoria* sp., CD9824	
Chalicotherium brevirostris, CD9823	
Cervidae indet., CD9824	
Artiodactyla indet., CD9816	
Proboscidea indet., CD9816	
Huaitoutala Fauna	Early Pliocene (4–5 Ma)
Mimomys sp., CD9822	
Orientalomys/*Chardinomys* sp., CD9822	
Micromys sp., CD9822	
Pseudomeriones sp., CD9822	
Soricidae indet., CD9822	

Numbers following taxonomic names are field numbers of the Institute of Vertebrate Paleontology and Paleoanthropology. For a more complete faunal list that includes mammals from other sections, see Wang et al. (in review).

of the NE Tibetan Plateau from models, basin analysis and thermochronology [3,7,8,10,13,18,23,36,41–45].

Specific evidence for event T1 includes field observations of the Honggouzi anticline in the northwest Qaidam Basin (Fig. 1) and seismostratigraphy of the Qaidam Basin demonstrate quite clearly that an unconformity occurs between the Shang Youshashan and Xia Youshashan Fms. close to the south slope of the Altyn Tagh and north margin of the Qaidam Basin. In our section, the first increase of sedimentation rate is also at the boundary of the Shang Youshashan and Xia Youshashan Fms. at 15.3 Ma accompanied by sharp changes in lithology from mostly fine sedimentary rocks of calcareous siltstone, mudstone and marl to predominantly coarse sedimentary rocks of sandstone intercalated with conglomerate (Figs. 8 and 9). In addition, rapid cooling of the rocks due to fast exhumation of the Qilian Shan and rapid rotation of the Guide Basin just east of the Qaidam Basin are recorded since the mid Miocene [46,47].

Specific evidence for event T2 at ~8.1 Ma starts at the bottom of the Shizigou Fm. and is characterized by an upward increase of thick sandstone in the section (Fig. 8), and of conglomerate in other sections over the margin of the Qaidam Basin. The predominance of alternating conglomerate and sandstone is the most marked feature of the Shizigou Fm. in the basin, and is indicative of rapid uplift of the surrounding mountains [1,2]. A number of tectonic deformation and uplift events at ~8 Ma have been reported around the Qaidam Basin and from various parts of the Tibetan Plateau, e.g. the Guide and Linxia Basins for the uplift of the east Kunlun Shan and west Qin Ling (Mts.) [36,41] (see Fig. 1 for locations); the Jiuquan Basin in the west Hexi Corridor for the uplift of the north Qilian Shan [44,48]; the Altyn Tagh from thermochronology [43,45]; the Kuche depression for uplift of the Tien Shan [33]; the Longmen Shan for uplift of east Tibet [49,50]; and the Yangbajing Basin for uplift of south Tibet [51].

The third sedimentation rate increase (event T3) at 3.6 Ma is not accompanied by a sharp lithologic change in the study section (even though the Quaternary section is completely dominated by conglomerate) (Figs. 8 and 9), but is synchronous with the occurrence of a growing stratum dipping from 67° to 45° within a narrow interval. This stratum is clearly indicative of a synchronous folding of the Keluke anticline by a backward propagation fault F_2 from backthrust F_2 due to a push by the southern Qilian Shan (Figs. 1 and 3). Seismostratigraphy confirms that this growth stratum is an overall feature around all margins of the Qaidam Basin [1,2]. An eastward fast shift of the depocenter of the Qaidam Basin was estimated to occur largely since the Plio-Quaternary [1,2,42]. Just to the north side of the Qilian Shan, an unconformity caused by the strong deformation from the Qilian Shan was paleomagnetically dated at ~3.7 Ma [44]. Huge and thick boulder conglomerate due to a tectonic uplift first appeared at about this time around the rim of the whole Tibetan Plateau [38,41,44,48,52,53], although a concurrent climatic change may also have contributed to this abrupt change [54]. Initiation of an E–W extension and graben system in northern Tibet and the formation of the Kunlun Pass Basin due to the strike–slip of the Kunlun fault and other strike–slip faults, and the basaltic eruption and fast cooling of granites on the eastern Tibetan Plateau due to rapid tectonic uplift and exhumation are all reported to occur at about this time [48,55–58].

The end of sedimentation in the study section at about 1.8 Ma is regarded as the strongest tectonic deformation due to the fast backward propagation of F_2 driven by rapid backthrusting of F_2, leading to the formation of the Keluke fault-propagation anticline. This anticline seems to be forming a clear step cutting the north limb of the anticline to the present. This fast

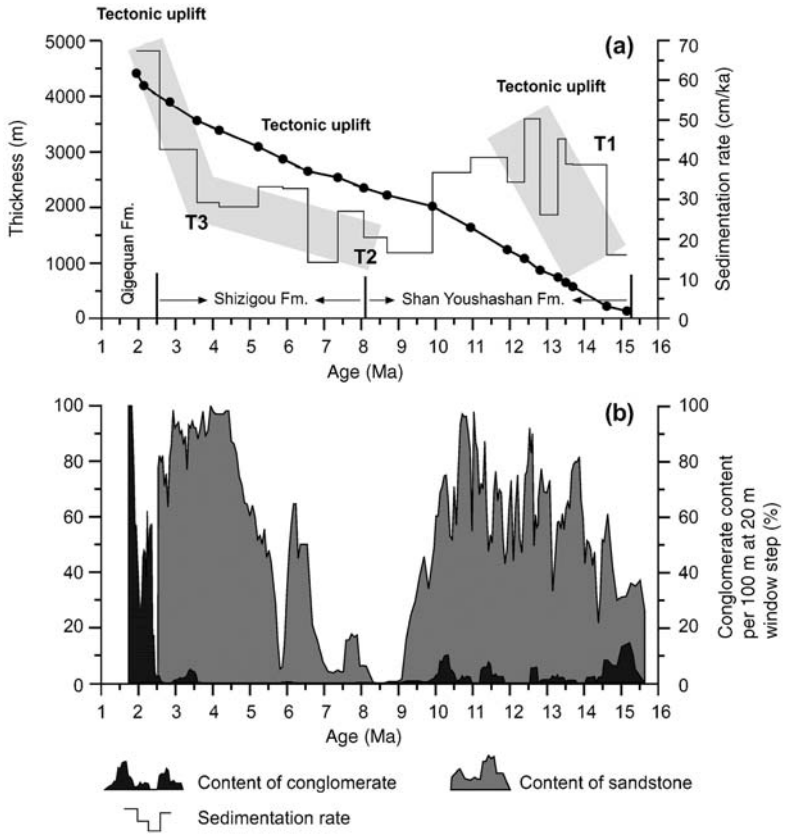

Fig. 9. (a) Thickness-vs.-age plots of the magnetic polarity chrons for the Huaitoutala section (with ages taken from the GPTS of Cande and Kent [29]). Sedimentation rates are plotted as well. The shaded zone indicates a persistent long-term increase of sedimentation rate which we interpret as a response to a tectonic uplift event (*T*). (b) Diagram showing the variation of percent occurrence of conglomerate and sandstone beds, calculated for each 100-m stratigraphic interval using 20-m moving window increments.

deformation and uplift is synchronous with the rapid fault-propagation folding of the Laojunmiao anticline with an unconformity in the Hexi Corridor to the north of the Qilian Shan, and the Ganjia and Yinchuangou anticlines and with great incision by the Yellow River in the Guide and Linxia Basins, respectively [36,41,44] (see Fig. 1 for localities).

6. Conclusions

Detailed paleomagnetic studies of the fossil mammal-bearing, 4570 m Huaitoutala section has yielded a high-resolution chronology for the stratigraphy of fossil mammals in the Qaidam Basin. This thick section was determined to have been recently formed between ~15.7 Ma and 1.8 Ma with the Shang Youshashan and the Shizigou formations falling in the intervals 15.3–8.1 Ma and 8.1–2.5 Ma and the Xia Youshashan Formation at >15.3 Ma, and the Qigequan Formation at <2.5 Ma. Three mammalian faunas, the Huaitoutala Fauna, the Tuosu Fauna, and the Olonbuluk Fauna, span the time periods of ~4.8 Ma, 9.5–11.4 Ma and 12.5–13.8Ma, respectively.

Our new chronology suggests a very high average sedimentation rate of ~33 cm/ka for the Huaitoutala section, which is also punctuated by three rapid increases starting at about ~14.7 Ma, 8.1 Ma and 3.6 Ma. These changes of sedimentation rate are concurrent with stratigraphic tilting and lithologic coarsening due to fault-propagation-folding, and are indicative of three episodes of rapid uplift and fast exhumation of the NE Tibetan Plateau at those times.

Acknowledgements

This study was co-supported by Chinese National Science Foundation Grants (nos. 40334038, 40421101, and 40128004), Sci. & Tech. Key Project of Ministry of Education of China (Grant no. 306016), Chinese National Key Project on Basic Research (grant 2005CB422001), President Fund and Innovation Program of the Chinese Academy of Sciences (grant no.

kzcx2-yw-104), Chinese Academy of Sciences Outstanding Overseas Scholars fund (KL205208), National Science Foundation (US) (EAR-0446699), and National Geographic Society (nos. 6004-97 and 6771-00). We thank Chen Yü, Wu Fuli, Wang Yadong, Li Lili, Xu Xianhai, Lu Xinchuan, Ma Wenzhong, Liu Shenchang, Wang Xin, Hu Xiaofei and Chang Huajin for field assistance, and Zhuang Guangsheng, Li Lili, Zan Jinbo, Liu Weiming and Fang Xiaohui for laboratory assistance. Special thanks are due to Professor Zhu Rixiang for his persistent laboratory support and to the Qinghai Petroleum Company of China National Petroleum Corporation for access to seismostratigraphic data.

References

[1] S. Gu, W. Xu, C. Xue, S. Di, F. Yang, H. Di, D. Zhao, Regional Petroleum Geology of Qinghai–Xizang Oil–Gas Field, vol. 14, Petroleum Publ. House, Beijing, 1990 (in Chinese with English title), 88 pp.

[2] H.C. Huang, Q.H. Huang, Y.S. Ma, Geology of Qaidam and Petroleum Prediction, Geological Publ. House, Beijing, 1996 (in Chinese) 257 pp.

[3] W.C. Xia, N. Zhang, X.P. Yuan, L.S. Fan, B.S. Zhang, Cenozoic Qaidam basin, China: a stronger tectonic inversed, extensional rifted basin, Am. Assoc. Pet. Geol. Bull. 85 (2001) 715–736.

[4] J.T. Wang, E. Derbyshire, J. Shaw, Preliminary magnetostratigraphy of Dabusan Lake, Qaidam Basin, central Asia, Phys. Earth Planet. Inter. 44 (1986) 41–46.

[5] Z.C. Liu, Y.J. Wang, Y. Chen, X.S. Li, Q.C. Li, Magnetostratigraphy and sedimentologically derived geochronology of the Quaternary lacustrine deposits of a 3000 m thick sequence in the central Qaidam basin, western China, Palaeogeogr. Palaeoclimatol. Palaeoecol. 140 (1998) 459–473.

[6] J. Wang, Y.J. Wang, Z.C. Liu, J.Q. Li, P. Xi, Cenozoic environmental evolution of the Qaidam Basin and its implications for the uplift of the Tibetan Plateau and the drying of central Asia, Palaeogeogr. Palaeoclimatol. Palaeoecol. 152 (1999) 37–47.

[7] F. Métivier, Y. Gaudemer, P. Tapponnier, B. Meyer, Northeastward growth of the Tibet plateau deduced from balanced reconstruction of two depositional areas – The Qaidam and Hexi Corridor basins, Tectonics 17 (1996) 823–842.

[8] P. Tapponnier, Z. Xu, F. Roger, B. Meyer, N. Arnaud, G. Wittlinger, J. Yang, Oblique stepwise rise and growth of the Tibet Plateau, Science 294 (2001) 1671–1677.

[9] B.C. Burchfiel, Q.D. Deng, P. Molnar, L. Royden, Y.P. Wang, P.Z. Zhang, Intracrustal detachment with zones of continental deformation, Geology 17 (1989) 448–452.

[10] B. Meyer, P. Tapponnier, L. Bourjot, F. Métivier, Y. Gaudemer, G. Peltzer, S. Guo, Z. Chen, Crustal thickening in Gansu–Qinghai, lithospheric mantle subduction, and oblique, strike–slip controlled growth of the Tibet Plateau, Geophys. J. Int. 135 (1998) 1–47.

[11] P. Molnar, P. Tapponnier, Cenozoic tectonics of Asia: effects of a continental collision, Science 189 (1975) 419–426.

[12] P. Tapponnier, P. Molnar, Active faulting and tectonics in China, J. Geophys. Res. 82 (B20) (1977) 2905–2930.

[13] A. Yin, P.E. Rumelhart, R. Butler, E. Cowgill, T.M. Harrison, D.A. Foster, R.V. Ingersoll, Q. Zang, X.Q. Zhou, X.F. Wang, A. Hanson, A. Raza, Tectonic history of the Altyn Tagh fault system in northern Tibet inferred from Cenozoic sedimentation, Geol. Soc. Amer. Bull. 114 (2002) 1257–1295.

[14] X. Wang, B.Y. Wang, Z.D. Qiu, W.R. Downs, G.P. Xie, Revisit Tsaidam Basin (late Tertiary) in northern Tibetan Plateau, J. Vertebr. Paleontol. 20 (2000) 76A.

[15] T. Deng, X. Wang, New material of the Neogene rhinocerotids from the Qaidam Basin in Qinghai, China, Vertebr. PalAsiat. 42 (2004) 216–229.

[16] T. Deng, X. Wang, Late Miocene Hipparion (Equidae, Mammalia) of eastern Qaidam Basin in Qinghai, China, Vertebr. PalAsiat. 42 (2004) 316–333.

[17] R.H. Tedford, Neogene mammalian biostratigraphy in China: past, present, and future, Vertebr. PalAsiat. 33 (1995) 272–289.

[18] B.D. Ritts, U. Biffi, Magnitude of post-Middle Jurassic (Bajocian) displacement on the central Altyn Tagh fault system, northwest China, Geol. Soc. Amer. Bull. 112 (1) (2000) 61–74.

[19] Q. Meng, J. Hu, F. Yang, Timing and magnitude of displacement on the Altyn Tagh fault: constraints from stratigraphic correlation of adjoining Tarim and Qaidam basins, NW China, Terra Nova 13 (2001) 86–91.

[20] Y. Chen, S. Gilder, N. Halim, J.P. Cogné, V. Courtillot, New paleomagnetic constraints on central Asian kinematics: displacement along the Altyn Tagh fault and rotation of the Qaidam Basin, Tectonics 21 (5) (2002) 1042, doi:10.1029/2001TC901030.

[21] P. Tapponnier, G. Peltzer, A.Y. Le Dain, R. Armijo, Propagating extrusion tectonics in Asia: new insights from simple experiments with plasticine, Geology 10 (1982) 611–617.

[22] G. Peltzer, P. Tapponnier, R. Armijo, Magnitude of late Quaternary left-lateral displacements along the north edge of Tibet, Science 246 (1989) 1285–1289.

[23] W.P. Chen, C.Y. Chen, J.L. Nábelek, Present-day deformation of the Qaidam basin with implications for intra-continental tectonics, Tectonophysics 305 (1999) 165–181.

[24] T. Song, X. Wang, Structural styles and stratigraphic patterns of syndepositional faults in a contractional setting: examples from Qaidam basin, northwestern China, Am. Assoc. Pet. Geol. Bull. 77 (1993) 102–117.

[25] L. Tauxe, Paleomagnetic Principles and Practice, Kluwer Academic Publishers, Dordrecht, 1998, 299 pp.

[26] M.W. McElhinny, Statistical significance of the Fold Test in Paleomagnetism, Geophys. J. R. Astron. Soc. (1964) 33–40.

[27] P.L. McFadden, A new fold test for paleomagnetic studies, Geophys. J. Int. 103 (1990) 163–169.

[28] L. Tauxe, Y. Gallet, A jackknife for magnetostratigraphy, Geophys. Res. Lett. 18 (1991) 1783–1786.

[29] S.C. Cande, D.V. Kent, Revised calibration of the geomagnetic polarity timescale for the Late Cretaceous and Cenozoic, J. Geophys. Res. 100 (1995) 6063–6095.

[30] Z. Qiu, W. Wu, Z. Qiu, Miocene mammal faunal sequences of China: palaeozoogeography and Eurasian relationships, in: G.E. Rössner, K. Heissig (Eds.), The Miocene Land Mammals of Europe, Dr. Driedrich Pfeil, München, 1999, pp. 443–472.

[31] Z.M. Sun, Z.Y. Yang, J.L. Pei, X.H. Ge, X.S. Wang, T.S. Yang, W.M. Li, S.H. Yuan, Magnetostratigraphy of Paleogene sediments from northern Qaidam Basin, China: implications for tectonic uplift and block rotation in northern Tibetan Plateau, Earth Planet. Sci. Lett. 237 (2005) 635–646.

[32] S. Dai, X.M. Fang, C.H. Song, J.P. Gao, D.L., J.J. Li, Early tectonic uplift of the northern Tibetan Plateau, Chin. Sci. Bull. 50 (2005) 1642–1652.

[33] B.C. Huang, D.A. John, S.T. Peng, T. Liu, Z. Li, Q.C. Wang, R.X. Zhu, Magnetostratigraphic study of the Kuche Depression, Tarim Basin, and Cenozoic uplift of the Tian Shan Range, Western China, Earth Planet. Sci. Lett. 251 (2006) 346–364.
[34] L. Yue, F. Heller, Z. Qui, L. Zhang, G. Xie, Z. Qiu, Y. Zhang, Magnetostratigraphy and paleoenvironmental record of Tertiary deposits of Lanzhou Basin, Chin. Sci. Bull. 46 (2001) 770–774.
[35] Z. Qiu, B. Wang, Z. Qiu, F. Heller, L. Yue, G. Xie, X. Wang, Land–mammal geochronology and magnetostratigraphy of mid-Tertiary deposits in the Lanzhou Basin, Gansu Province, China, Ecol. Geol. Helv. 94 (2001) 373–385.
[36] X.M. Fang, C. Garzione, R. Van der Voo, J.J. Li, M.J. Fan, Flexural subsidence by 29 Ma on the NE edge of Tibet from the magnetostratigraphy of Linxia Basin, China, Earth Planet. Sci. Lett. 210 (2003) 545–560.
[37] S. Dai, X.M. Fang, G. Dupont-Nivet, C.H. Song, J.P. Gao, W. Krijgsman, C. Langereis, W.L. Zhang, High resolution magnetostratigraphy of Cenozoic sediments in Xining Basin and its implication on tectonic deformation and uplift of the northeastern Tibetan Plateau, J. Geophys. Res. 111 (2006), doi:10.1029/2005JB004187.
[38] H.B. Zheng, C.M. Powell, Z.S. An, J. Zhou, G.R. Dong, Pliocene uplift of the northern Tibetan Plateau, Geology 28 (2000) 715–718.
[39] Z.J. Zhao, X.M. Fang, J.J. Li, et al., Paleomagnetic dating of the Jiuquan Gravel in the Hexi Corridor: implication on the mid-Pleistocene uplift of the Qinghai–Tibetan Plateau, Chin. Sci. Bull. 46 (14) (2001) 1208–1212.
[40] J. Chen, D.W. Burbank, K.M. Scharer, E. Sobel, J.H. Yin, C. Rubin, R.B. Zhao, Magnetochronology of the Upper Cenozoic strata in the southwestern Chinese Tian Shan: rates of Pleistocene folding and thrusting, Earth Planet. Sci. Lett. 195 (2002) 113–130.
[41] X.M. Fang, M.D. Yan, R. Van der Voo, D.K. Rea, C.H. Song, J.M. Pares, J.S. Nile, J.P. Gao, S. Dai, Late Cenozoic deformation and uplift of the NE Tibetan Plateau: evidence from high-resolution magnetostratigraphy of the Guide Basin, Qinghai Province, China, Geol. Soc. Amer. Bull. 117 (2005) 1208–1225.
[42] Q. Wang, M.P. Coward, The Chaidam basin (NW China): formation and hydrocarbon potential, J. Pet. Geol. 13 (1990) 93–112.
[43] M. Jolivet, M. Brunel, D. Seward, Z. Xu, J. Yang, F. Roger, P. Tapponnier, J. Malavielle, N. Arnaud, C. Wu, Mesozoic and Cenozoic tectonics of the northern edge of the Tibetan Plateau: fission tract constraints, Tectonophysics 343 (2001) 111–134.
[44] X.M. Fang, Z.J. Zhao, J.J. Li, M.D. Yan, B.T. Pan, C.H. Song, S. Dai, Magnetostratigraphy of the late Cenozoic Laojunmiao anticline in the northern Qilian Mountains and its implications for the northern Tibetan Plateau uplift, Sci. China, Ser. D: Earth Sci. 48 (2005) 1040–1051.
[45] Z.L. Chen, X.F. Wang, A. Yin, B.L. Chen, X.H. Chen, Cenozoic left-slip motion along the central Altyn Tagh Fault as inferred from the sedimentary record, Int. Geol. Rev. 46 (2004) 839–856.
[46] A.D. George, S.J. Marshallsea, K. Wyrwoll, J. Chen, Y. Lu, Miocene cooling in the northern Qilian Shan, northeastern margin of the Tibetan Plateau, revealed by apatite fission-track and vitrinite-reflectance analysis, Geology 29 (2001) 939–942.
[47] M.D. Yan, R. Van der Voo, X.M. Fang, J.M. Parés, D.K. Rea, Paleomagnetic evidence for a mid-Miocene clockwise rotation of about 25 of the Guide Basin area in NE Tibet, Earth Planet. Sci. Lett. 241 (2006) 234–247.
[48] C.H. Song, X.M. Fang, J.J. Li, J.P. Gao, M.J. Fan, Tectonic uplift and sedimentary evolution of the Jiuxi Basin in the northern margin of the Tibetan Plateau since 13 Ma Bp, Sci. China, Ser. D: Earth Sci. 44 (2001) 192–202 (Suppl.).
[49] E. Kirby, P. Reiners, M. Krol, K. Hodges, K. Whipple, K. Farley, W. Tang, Z. Chen, Late Cenozoic uplift and landscape evolution along the eastern margin of the Tibetan Plateau: inferences from $^{40}Ar/^{39}Ar$ and (U–Th)/He thermochronology, Tectonics 21 (1) (2002) 1001, doi:10.1029/2000TC001246.
[50] P. Molnar, Mio-Pliocene growth of the Tibetan Plateau and evolution of East Asian climate, Palaeontol. Electronica 8 (1) (2005) 1–23.
[51] T.M. Harrison, P. Copeland, W.S.F. Kidd, A. Yin, Raising Tibet, Science 255 (1992) 1663–1670.
[52] D.W. Burbank, G.D. Johnson, Intermontane-basin development in the past 4 Myr in the north-west Himalayas, Nature 298 (1982) 432–436.
[53] J.J. Li, X.M. Fang, R. Van der Voo, J.J. Zhu, C. MacNiocaill, J.X. Cao, W. Zhong, H.L. Chen, J.L. Wang, J.M. Wang, Y.T. Zhang, Late Cenozoic magnetostratigraphy (11–0 Ma) of the Dongshanding and Wangjiashan sections in Longzhong Basin, western China, Geol. Mijnb. 76 (1997) 121–134.
[54] P. Zhang, P. Molnar, W.R. Downs, Increased sedimentation rates and grain sizes 2–4 Myr ago due to the influence of climate change on erosion rates, Nature 410 (2001) 891–897.
[55] A. Yin, P.A. Kapp, E. Craig, T. Mark Harrison, M. Grove, L. Ding, X.G. Deng, C.M. Wu, Significant late Neogene east–west extension in northern Tibet, Geology 27 (1999) 787–790.
[56] J.J. Li, X.M. Fang, B.T. Pan, Z.J. Zhao, Y.G. Song, Late Cenozoic intensive uplift of Qinghai–Xizang Plateau and its impacts on environments in surrounding area (in Chinese with English abstract), Quat. Sci. 21 (5) (2001) 381–390.
[57] E. Kirby, K.X. Whipple, W.Q. Tang, Z.L. Chen, Distribution of active rock uplift along the eastern margin of the Tibetan Plateau: inferences from bedrock channel longitudinal profiles, J. Geophys. Res. 108 (B4) (2003) 2217, doi:10.1029/2001JB000861.
[58] C.H. Song, D.L. Gao, X.M. Fang, Z.J. Cui, J.J. Li, S.L. Yang, H.B. Jin, D. Burbank, J.L. Kirschvink, High-resolution magnetostratigraphy of late Cenozoic sediments from the Kunlun Shan Pass Basin and its implications on deformation and uplift of the northern Tibetan Plateau, Chin. Sci. Bull. 50 (17) (2005) 1912–1922.